Desalination and Water Treatment
www.deswater.com

doi: 10.5004/dwt.2017.20314

65 (2017) 284–293
February

Preparation of polymeric aluminum ferric silicate for the pre-treatment of oily wastewater through response surface method

Mengdan Tang[a], Yongjun Sun[a,b,*], Chengyu Zhu[a], Yanhua Xu[b], Huaili Zheng[c], Xuefeng Xiao[a], Wenquan Sun[a], Huifang Wu[a], Cuiyun Liu[a]

[a]*College of Urban Construction, Nanjing Tech University, Nanjing, 211800, China, emails: sunyongjun008@163.com (Y. Sun), sunyongjun@njtech.edu.cn (Y. Sun), 935763168@qq.com (M. Tang), 2506885738@qq.com (C. Zhu), xuefengnjut@163.com (X. Xiao), coneflower@163.com (W. Sun), wuhuifang@163.com (H. Wu), yunduobai@126.com (C. Liu)*
[b]*Jiangsu Key Laboratory of Industrial Water-Conservation & Emission Reduction, College of Environmental Science and Engineering, Nanjing Tech University, Nanjing, 211800, China, email: yanhuaxu18@hotmail.com*
[c]*Key laboratory of the Three Gorges Reservoir Region's Eco-Environment, State Ministry of Education, Chongqing University, Chongqing, 400045, China, email: zhl@cqu.edu.cn*

Received 26 May 2016; Accepted 29 October 2016

ABSTRACT

A new composite coagulant, polymeric aluminum ferric silicate (PAFSi), was prepared for the pre-treatment of oil-containing wastewater. The structure and morphology of PAFSi were investigated through X-ray diffraction, Fourier transform infrared spectroscopy, and scanning electron microscopy. Results revealed that PAFSi is a new complex multi-hydroxyl polymeric coagulant rather than a simple mixture of raw materials. Response surface method was applied to optimize the preparation process. Optimization performance was evaluated according to flocculation efficiency. The flocculation efficiency of PAFSi was determined by measuring the reduction in oil and chemical oxygen demand (COD). In addition, the parameters that affect flocculation efficiency, such as coagulant dosage and oily wastewater initial pH, were examined. Compared with polymeric aluminum ferric sulfate (PAFS), PAFSi exhibited superior flocculation performance, with maximum oil removal efficiency of 96.9% and maximum COD removal efficiency of 95.4% at a dosage of 25 mg·L^{-1} and pH of 7. PAFSi exhibited better flocculation ability than PAFS.

Keywords: Composite coagulant; Coagulation; Response surface methodology; Oily wastewater; Oil removal

1. Introduction

Industrial development has increased the consumption of oil. A large amount of oily wastewater is discharged into rivers and oceans because of the high cost and ineffective management of oily wastewater treatment; as a result, environmental contamination occurs [1]. Oily wastewater originates from numerous sources, and large amounts of oily wastewater are produced during oil production, oil refining, oil storage, transportation and petrochemical activities, and fuel consumption [2]. The pollution prevention equipment for machinery space bilges of ships has elicited much attention because of the increasing demand for marine environmental protection. Oily bilge water from ships includes soiled and machine washing wastewater. Ships as maritime trade transport vessels bring economic development, but they inevitably affect the marine environment [3]. The oil pollution caused by ships to the marine environment is particularly serious and has become an important issue worldwide [4]. Oil pollution by ships occurs in the form of illegal discharge of oily pollutants during operation. With its characteristics of extensive sources, complex components, and poor biodegradability, oily wastewater causes much harm to ecosystems and the water environment [5]. Ineffective oil pollution

* Corresponding author.

control can result in long-term negative effects on the marine environment. Currently, many measures are adopted to deal with oily bilge water and satisfy the requirements of MEPC.107(49), which was established by the International Maritime Organization.

The high oil content, chemical oxygen demand (COD), and turbidity as well as the complex components of oily wastewater make reaching the discharge standard at a low cost difficult [6]. Currently, the methods for treating oily wastewater, such as flotation [7], flocculation [8], electrochemical method [9], membrane separation [10], biological method [11], and physical chemical treatment [12], are developing rapidly. However, these methods have limitations, such as high cost, low oil removal efficiency, and easy corrosion of equipment [13]. The method of flocculation–coagulation has been widely utilized for the pre-treatment of oily wastewater because of its fast reaction, short settling time, high removal efficiency of oil content, and simple operation [14]. When coagulants are dosed into oily wastewater, fine oil drops and colloidal suspensions destabilize, collide, flocculate, and then aggregate into large flocs through charge neutralization and adsorption bridging. Ultimately, aggregated flocs are separated by gravity precipitation to achieve solid–liquid separation and oil removal [15,16].

In practical applications, the selection of an appropriate coagulant for the treatment of oil wastewater plays a crucial role in oil removal efficiency [17]. Inorganic polymer coagulants, such as polyaluminum chloride and polymeric ferric sulfate, have better flocculation efficiency, lower dosage, and less sludge flocs than inorganic coagulants with a low molecular weight, such as aluminum sulfate and ferric chloride. Meanwhile, organic polymer flocculants are often used as flocculation additives because of their high cost [18]. Most oily wastewater treatment stations use polyaluminum chloride and polymeric ferric sulfate as coagulants because of their good coagulation performance. However, these products have high dosage, slow sedimentation rate, and poor purification effect [19]. Considerable interest has been provided to the development and potential use of polysilicate with the capacity for flocculation [20]. Polysilicate as a coagulant is an excellent inorganic polymer coagulant compared with traditional inorganic coagulants in many aspects, such as large flocs, rapid settlement, wide applicable pH range, and low cost [21,22]. Meanwhile, the composite reactions of certain highly charged metal ions (iron and aluminum) and polysilicate can improve its charge neutralization capacity and absorption bridging ability, thus increasing its flocculation property [23,24].

In this study, polymeric aluminum ferric silicate (PAFSi) was prepared for the pre-treatment of oily wastewater. To optimize the preparation condition, Si/Fe, Al/Fe, OH/Fe, and pH, which may affect residual oil concentration, were investigated. Response surface methodology (RSM) was employed to investigate the mutual effect and obtain the optimum preparation conditions. PAFSi was then characterized through X-ray diffraction (XRD) analysis, Fourier transform infrared (FTIR) spectroscopy, and scanning electron microscopy (SEM) to investigate its structural characteristics. The effects of coagulant dosage and oily wastewater initial pH on flocculation performance were systematically evaluated.

2. Experimental setup

2.1. Materials

All reagents used in this study were of analytical grade, except for ferrous sulfate ($FeSO_4 \cdot 7H_2O$), which was of technical grade. All aqueous and standard solutions were prepared with deionized water. All reagents were purchased from Nanjing SHENGJIANQUAN Chemical Glassware Instrument Co., Ltd (Nanjing, China). All reagents were used in the experiment without further purification.

2.2. Preparation of PAFSi

A series of PAFSi were prepared in the laboratory. First, 50–70 g of $FeSO_4 \cdot 7H_2O$ was oxidized with sodium chlorate and gradually stirred in a beaker until a homogeneous liquid mixture was obtained. A measured amount of $Al_2(SO4)_3$ (Al/Fe = 0.5:1 – 1.5:1) solution was added to the reaction vessel to prepare a new liquid mixture containing aluminum and iron. The new liquid mixture was then stirred gradually for 30 min in a thermostatic water bath at a temperature of 70°C to improve the hydrolysis and polymerization reactions. Second, a measured amount of polysilicic acid with Si/Fe = 1:1 – 1:8 was added to the aluminum–iron solution. Third, Na_2CO_3 was added to the aluminum–iron solution with polysilicic acid to obtain the desired *r* value (*r* is the OH/Fe molar ratio) and improve its stability. PAFSi was obtained after stirring for 120 min in a thermostatic water bath.

2.3. Characterizations of PAFSi

The powder of PAFSi was characterized through XRD to determine the crystalline phases; a D/Max-3C X-ray diffractometer (ARL X'TRA, America) was used in the range of 10°–80° (2θ) and at a scan rate of 4°/min. FTIR spectra were obtained with a 550 Series II infrared spectrometer (Bruker Company, Switzerland) through the potassium bromide disc technique. SEM of the PAFSi was conducted with a VEGA II LMU SEM system (TES-CAN Company, Czech Republic). The fractal dimension was the linear correlation of the logarithm of projected area (*A*) and the characteristic length (*L*), and the fractal dimension can be calculated from reference [25].

2.4. Coagulation tests and optimization design of the preparation process

The simulated oil-containing wastewater was prepared with oil and surfactant according to the method in MEPC.107(49). The original water quality of the simulated oil-containing wastewater was 10,670 mg·L^{-1} COD, 2,548 mg/L oil, and pH of 7. The oil content of the wastewater was measured according to the petroleum and natural gas industry standard (SY/T0530-93) of People's Republic of China. Oil content as a function of absorbance at 256 nm can be expressed by the standard equation y = 0.29185x – 0.0563 (R^2 = 0.9999). Oil content was calculated via the standard equation.

All coagulation experiments were conducted in 1.0 L glass beakers and with a program-controlled jar-test apparatus (ZR4-6, Zhongrun Water Industry Technology Development Co., Ltd., China) operating at room temperature. The pH of

the simulated oil-containing wastewater was adjusted with HCl (0.1 mol·L^{-1}) or NaOH (0.1 mol·L^{-1}). The dosage of PAFSi was 30 mg/L in the four-factor Box–Behnken design. All the dosages of different coagulants are calculated by their dry weight in the flocculation tests. Before the rapid stirring phase, a measured amount of coagulant was pipetted into the wastewater sample (1.0 L). The wastewater samples were mixed rapidly at 350 rpm for 3 min after dosing, followed by slow stirring at 80 rpm for 5 min and sedimentation for 15 min. After sedimentation, supernatant samples were collected 2 cm below the water surface of the wastewater samples to measure oil content, turbidity (2100Q turbidimeter, Hach, USA), and COD (DR/5000 UV spectrophotometer, Hach, USA).

To obtain the optimum preparation process, RSM was utilized to optimize the preparation process through performance optimization evaluation. Three significant levels of coagulant properties that affect coagulation–flocculation efficiency were selected for the statistical method and Box–Behnken experimental designs to investigate the mutual influence of factors on flocculation efficiency [26]. The experimental results indicating the significant levels are shown in Table 1. Factor levels were selected in such a manner that the upper level corresponds to +1, the lower level to –1, and the basic level to 0.

To decide the optimum preparation conditions, establish a model for the preparation of PAFSi, and investigate the effect of coagulant components on coagulation performance, four significant levels for the preparation process factors were selected for the statistical method and Box–Behnken experimental designs. The mutual influence of the impact factors on residual oil concentration was investigated. The experimental results were analyzed with a professional software, Design-Expert V8.0, which employs the quadratic equation model to show the effects of factors in terms of linear, quadratic, and cross-product terms [27]:

$$Y = \beta_0 + \sum_{i=1}^{f} \beta_i X_i + \sum_{i=1}^{f} \beta_{ii} X_i^2 + \sum_{i,s1}^{f} \sum_{j}^{f} \beta_{ij} X_i X_j + \varepsilon \quad (1)$$

where Y, f, β_0, β_i, x_i, β_{ii}, β_{ij}, and ε represent the dependent variables (residual oil concentration), number of variables, constant term, coefficients of the linear parameters, variables, coefficients of the quadratic parameters, coefficients of the interaction parameters, and residual associated with the experiments, respectively. Table 1 presents the experimental ranges and levels of the independent test variables. Residual oil concentration was selected as the response value (dependent variable). The investigation was conducted through 29 experimental runs, as presented in Table 2.

Table 1
Experimental ranges and levels of the independent test variables

Variables	Ranges and levels		
	–1	0	+1
Si/Fe (X_1)	1:1	1:4	1:8
Al/Fe (X_2)	0.5:1	1:1	1.5:1
OH^-/Fe (X_3)	0.1	0.3	0.5
pH (X_4)	0.5	2	3.5

3. Results and discussion

3.1. XRD spectrum

As revealed by the XRD patterns in Fig. 1, the main characteristic diffraction peaks distributed in 2θ = 10°–40° inidicate a Keggin structure [28,29]. Similar Al_{13} structures were formed in PAFSi. As shown in Fig. 1, the crystallinity of polymeric aluminum ferric silicate (PAFS) was higher than that of PAFSi in the range of 2θ = 10°–30°. However, the crystallinity of PAFSi was higher than that of PAFS in the range of 2θ = 30°–40°. The introduction of Si obviously enhanced the structure of PAFSi toward amorphous state aggregation. Al and Fe ions were complexed by activated silicic acid to form complex composite polymers. Meanwhile, different hydroxyls at exposed terminated groups of polysilicates reacted with Al^{3+}, Fe^{3+}, and their hydrolysis products to inhibit the autopolymerization of silicate molecules and prevent the formation of polysilicic acid gel. These reactions can improve the molecular weight and stability of PAFi to some extent. Moreover, the addition of silicic acid changed the manner of accumulation and crystallization of the original polymeric ferric sulfate and facilitated the formation of a new multi-hydroxyl polymer. Compared with polymeric ferric sulfate, PAFSi had better stability during long-term storage.

3.2. FTIR spectrum

Fig. 2 shows the FTIR spectrum of PAFS and PAFSi. The absorption band observed at 3,387 and 3,601 cm^{-1} originated from the strong stretching vibration of hydroxyl groups, including hydroxyl groups in polysilicic acid and hydroxyl groups attached to Al and Fe. The Fe and Al ions reacted with polysilicic acid to form a polyhydroxy-containing alumina–silica (iron–silica) composite polymer [30]. The absorption peak at 1,632 cm^{-1} was mainly attributed to Al–O and Fe–O bonds. The absorption peaks at 1,150–1,270 cm^{-1} represented the bending vibration of coordinated water and crystal water in the structure of Al–OH–Al and Fe–OH–Fe. The bending vibration absorption peak of Fe–O–Si and Al–O–Si appeared at 1,018 cm^{-1}. The absorption peak at 618 cm^{-1} was attributed to the stretching vibration of Al(Fe)–OH(Si–OH) [31]. Compared with the IR spectra of PAFS, those of PAFSi had many new chemical bonds, indicating that silicic acid was involved in the polymerization reaction to prepare PAFSi. FTIR analysis demonstrated that the activated silicate reacted with iron and aluminum ions to form PAFSi.

3.3. SEM results

Fig. 3 shows the SEM photographs of PAFS and PAFSi. In the size range of 100 μm, PAFS was significantly larger than PAFSi. In the size range of 20 μm, they presented a different structure. PAFS presented a compact gel network structure (Fig. 3(a)), whereas PAFSi presented a branched and flake structure shown in Fig. 3(b). Compared with that of PAFS, the structure of PAFSi was more compact and flaky. This result indicates that the structure had a large specific surface area, and its absorption and bridging effect for destabilizing colloidal particles was strengthened. The differences between PAFS and PAFSi in terms of structure were due to the introduction of silicic acid in the preparation process.

Table 2
Four-factor Box–Behnken design and value of the response function [η]

Run order	Coded variables				Residual oil concentration ($mg·L^{-1}$)		Oil removal rate (%)	Residual COD concentration ($mg·L^{-1}$)	COD removal rate (%)	Residual turbidity
	X_1	X_2	X_3	X_4	Actual value	Predicted value				
1	1	1	0	0	389.2	387.6	84.73	994.8	90.68%	903
2	0	0	0	0	274.9	277.3	89.21	717.9	93.27%	543
3	0	0	0	0	277.4	277.3	89.11	719.8	93.25%	545
4	–1	1	0	0	150.1	148.1	94.11	191.1	98.21%	81.1
5	0	0	0	0	278.5	277.2	89.07	716.4	93.29%	542
6	0	1	0	–1	380.2	383	85.08	954.2	91.06%	118.4
7	0	0	1	1	248.3	244.8	90.26	1,666	84.39%	1,440
8	1	0	0	–1	465.1	463.3	81.75	1,205	88.71%	173
9	–1	–1	0	0	285.3	282.7	88.80	688.5	93.55%	393
10	0	0	–1	–1	299.6	298.9	88.24	1,109.5	89.60%	437
11	–1	0	0	–1	370.4	369.4	85.46	489.5	95.41%	228
12	0	1	0	1	309.4	311.8	87.86	947.6	91.12%	148.4
13	0	–1	0	–1	366.2	368.9	85.63	1,068.5	89.99%	191
14	0	1	1	0	278.4	278.4	89.07	889.2	91.67%	435
15	–1	0	1	0	248.2	250.4	90.26	798.5	92.52%	206
16	1	–1	0	0	300.1	297.9	88.22	898.5	91.58%	375
17	1	0	1	0	396.2	398.7	84.45	1,087.6	89.81%	228
18	–1	0	–1	0	288.1	290.8	88.69	809.2	92.42%	218
19	1	0	–1	0	394.2	397.2	84.53	1,109.3	89.60%	248
20	0	–1	0	1	368.4	370.8	85.54	1,079.9	89.88%	307
21	0	0	0	0	278.5	277.3	89.07	718.4	93.27%	548
22	1	0	0	1	462.1	462.1	81.86	1,178	88.96%	163
23	0	0	0	0	277.1	277.3	89.12	719.2	93.26%	544
24	0	–1	–1	0	321.4	320.4	87.43	1,102.3	89.67%	217
25	0	–1	1	0	289.3	289.9	88.65	912.4	91.45%	448
26	0	1	–1	0	288.5	286.8	88.68	890.9	91.65%	423
27	0	0	–1	1	550.5	548.2	78.39	1,489.3	86.04%	1,033
28	0	0	1	–1	565.3	563.4	77.81	1,298.4	87.83%	484
29	–1	0	0	1	300.4	301.2	88.21	478.3	95.52%	218

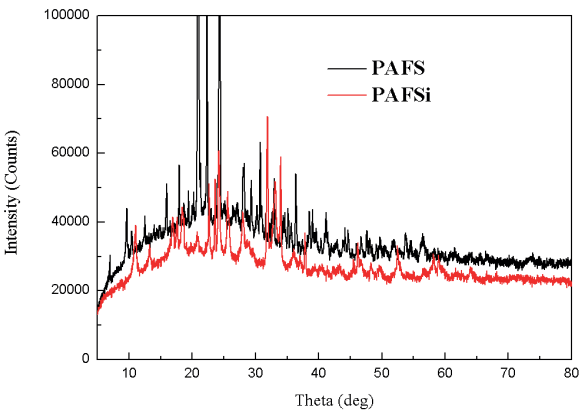

Fig. 1. XRD spectrum of PAFS and PAFSi.

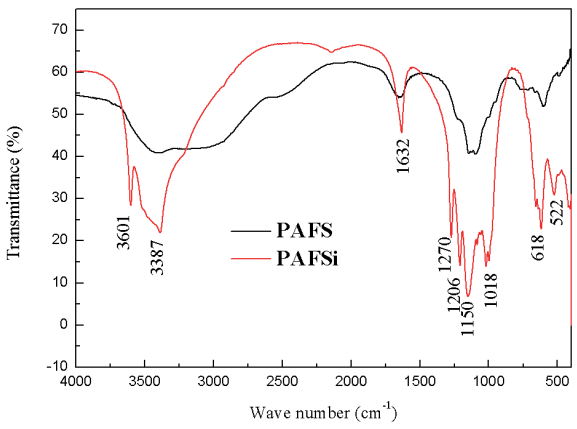

Fig. 2. FTIR spectrum of PAFS and PAFSi.

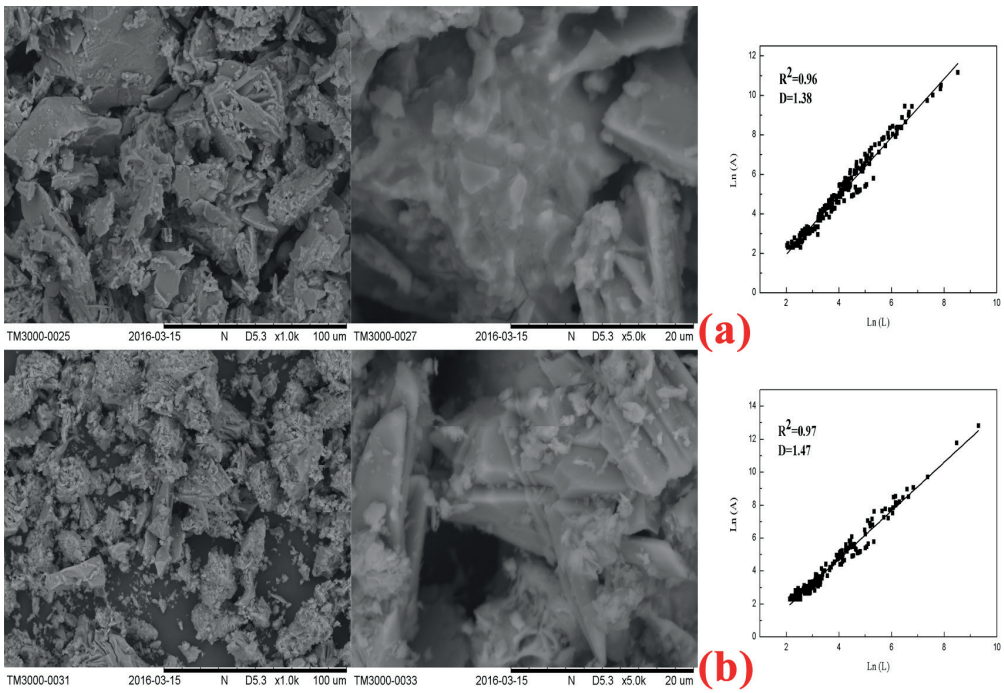

Fig. 3. SEM photographs of (a) PAFS and (b) PAFSi.

The flake structure of PAFSi resulted in improved stability in the case of long storage time. A linear correlation between the logarithm of perimeter (L) and area (A) was observed from the results of fractal dimension calculated using Image-Pro Plus 6.0 software. The average fractal dimensions of PAFS and PAFSi were 1.38 and 1.47, respectively. The discrepancy in fractal dimensions was due to the structure of PAFS and PAFSi; PAFSi with higher fractal dimensions had better flocculation ability [32,33].

3.4. Model fitting

Through RSM, Box–Behnken experimental designs were selected for the optimization and modeling of P(AM-DAC-BA) preparation, with X_1, X_2, X_3, and X_4 representing Si/Fe, Al/Fe, OH^-/Fe, and pH, respectively. The experimental ranges and levels of the independent test variables are shown in Table 1. Twenty-nine observed responses (Table 2) were utilized to calculate the model with the Box–Behnken method. From the experimental data, quadratic regression models were established with Design Expert V8.0.6, as shown in Eq. 2:

$$\text{Residual oil concentration} = +277.28 + 63.70\,X_1 - 11.24 - 9.72\,X_3 - 17.31\,X_4 + 56.07\,X_1X_2 + 10.47\,X_1X_3 + 16.75\,X_1X_4 + 5.50\,X_2X_3 - 18.25\,X_2X_4 - 141.97\,X_3X_4 + 21.08\,X_1^2 - 19.28\,X_2^2 + 35.91\,X_3^2 + 100.64\,X_4^2 \quad (2)$$

The adequacy of the models was investigated through analysis of variance (ANOVA), and the results are shown in Table 3. The F value of the model was 2,064.6, and the p value was less than 0.0001. These values indicate that the model is significant. The determination coefficient value, $R^2 = 0.9950$, indicated that the sample variation was 99.50% for residual oil concentration. This result is attributed to the independent variables; meanwhile, only 0.50% of the total variations were not explained by the model. Hence, a strong correlation exists between the predicted and observed values. Furthermore, a relatively low value of the coefficient of variation, CV = 0.84%, was obtained. This low value reveals the good precision and reliability of the performed experiments [34]. The above investigation shows that the model is adequate for the prediction of residual oil concentration.

3.5. Mutual effect of parameters

The purpose of this experiment is to observe the integrated effects of Si/Fe, Al/Fe, OH^-/Fe, and pH on residual oil concentration through the Box–Behnken statistical method. The experimental runs are presented in Table 2, which also shows oil removal rate, residual COD concentration, COD removal rate, and residual turbidity. Table 2 shows that the oil removal rate was in the range of 77.81%–94.11%. This range indicates that PAFSi had good flocculation ability for the removal of oil. Meanwhile, the removal rate of COD was in the range of 84.39%–98.21%. The highest COD removal rate was 98.21% at experimental run 4, with a residual COD concentration of 191.1 mg·L^{-1} and residual turbidity of 81.1 NTU. The experimental results in Table 2 show that PAFSi has good flocculation efficiency in removing COD and oil from oily wastewater.

To investigate the various factors and their mutual effects on residual oil concentration flocculated by PAFSi, response surface plots were utilized to display the response as a function of two factors. By keeping the remaining two factors constant, 2D response surface contours were plotted to analyze the mutual effect of operational variables. The response surface contour plots are shown in Fig. 4.

Table 3
ANOVA results for response parameters

Source	Sum of squares	Degrees of freedom	Mean square	*F* value	*p* value
Model	230,552	14	16,468.0	2,064.6	<0.0001
Si/Fe	48,692.3	1	48,692.3	6,104.6	<0.0001
Al/Fe	1,516.5	1	1,516.5	190.1	<0.0001
OH^-/Fe	1,133.0	1	1,133.0	142.0	<0.0001
pH	3,595.0	1	3,594.9	450.7	<0.0001
Residual	111.7	14	8.0		
Lack of fit	103.0	10	10.3	4.7	0.0735
Pure error	8.7	4	2.2		
Total	230,663.7	28			
R^2	0.9950				
R^2 adjusted	0.9990				

Fig. 4(a) shows the residual oil concentration as a function of Si/Fe and Al/Fe. Fig. 4(b) shows the residual oil concentration as a function of Si/Fe and OH^-/Fe (basicity). Fig. 4(c) shows the residual oil concentration as a function of Si/Fe and pH. Figs. 4(b) and 4(c) present the mutual effect of Si/Fe, Al/Fe, OH^-/Fe (basicity), and pH on the residual oil concentration. A decrease in Si/Fe resulted in a decrease in the residual oil concentration, especially with pH and OH^-/Fe (basicity) in the range of –0.5–0.5. Fig. 4(d) shows residual oil concentration as a function of OH^-/Fe (basicity) and pH. Fig. 4(e) shows residual oil concentration as a function of Al/Fe and pH. Fig. 1(f) shows residual oil concentration as a function of OH^-/Fe (basicity) and pH. An optimum circular region was observed within the mutual influence of two factors (Si/Fe and basicity; Si/Fe and pH), which were at –1.25–2.75 and 0.2–0.4 for pH and OH^-/Fe (basicity), respectively.

The mutual effect of Si/Fe, Al/Fe, OH^-/Fe (basicity), and pH within the investigated range demonstrated a positive role in enhancing flocculation efficiency [35]. The response optimizer in the Design Expert V8.0 software was used to search for an optimum preparation condition of PAFSi. In theory, the best condition for residual oil concentration is Si/Fe of 1:1.36, Al/Fe of 1:7.92, OH^-/Fe (basicity) of 0.34, and pH of 2.38.

3.6. Confirmation of the experimental results

To confirm the validity of the statistical experimental strategies, additional confirmation experiments were conducted in duplicate. The selected conditions for Si/Fe, Al/Fe, OH^-/Fe, and pH are listed in Table 4, along with the predicted and measured results. The table shows that the measured residual oil concentration was close to the values predicted with the regression model. This result indicates the suitability of the fitted polynomial models with respect to the experimental data. Data were confirmed to be significant by using this modeling regression method. Thus, PAFSi is effective in predicting residual oil concentration [36].

3.7. Effect of dosage on the removal of COD and oil

Figs. 5(a) and (b) show the effects of PAFSi and PAFS dosage on the flocculation efficiency of oily wastewater, respectively. Fig. 5(a) shows the effect of PAFSi and PAFS on the removal of COD. As the coagulant dosage increased from 10 to 35 $mg \cdot L^{-1}$, a decrease was observed in the level of residual COD concentration, and thus, an increase in the level of COD removal efficiency. When the coagulant dosage was more than 35 $mg \cdot L^{-1}$, the COD removal rate appeared to be stable at 95.4% and 87.8% for PAFSi and PAFS, respectively. Fig. 5(b) shows that oil removal efficiency increased along with coagulant dosage. Oil removal efficiency reached 95.0% and 82.2% at coagulant dosages of 25 and 35 $mg \cdot L^{-1}$ for PAFSi and PAFS, respectively. Meanwhile, when the dosage was more than 25 and 35 $mg \cdot L^{-1}$ for PAFSi and PAFS, respectively, the removal rate of oil began to achieve the maximum values of residual oil concentration of 127.4 and 453.4 $mg \cdot L^{-1}$, respectively. The comparison of COD and oil removal ability shown in Fig. 5 demonstrates that PAFSi had better flocculation performance than PAFS. Therefore, the optimal dosage of PAFSi for high concentration oil-containing wastewater treatment was determined to be 25 $mg \cdot L^{-1}$.

The coagulant was dissolved in water to form a large number of positively charged colloidal alumina–silica–iron-based polymers [37]. The dissolved coagulants quickly destroyed the stability of the original colloidal systems and neutralized the negatively charged oil droplets dispersed in the wastewater effectively [38]. Furthermore, the chain-type structure formed PAFS, which could adsorb and bridge the suspended colloid particles and the oil drops, thus aggregating them into large flocs. Hence, the oil drops and suspended colloid particles were easy to precipitate and remove from the water in the form of flocs by using PAFSi [39]. As shown in Fig. 6, PAFSi exhibited excellent purification performance for the treatment of high-concentration oil-containing wastewater. The zeta potential of wastewater was often used as a tool to investigate the charge neutralization performance of different inorganic coagulants. We have conducted several additional experiments. The zeta potentials of PAFSi at 20 and 40 mg/L were –22.3 and –14.6 mV, respectively. While the zeta potentials of PAFS at 20 and 40 mg/L were –25.0 and –21.2 mV, respectively. The zeta potential obtained by PAFSi was significantly higher than those obtained by PAFS, indicating PAFSi better charge neutralization performance than PAFS.

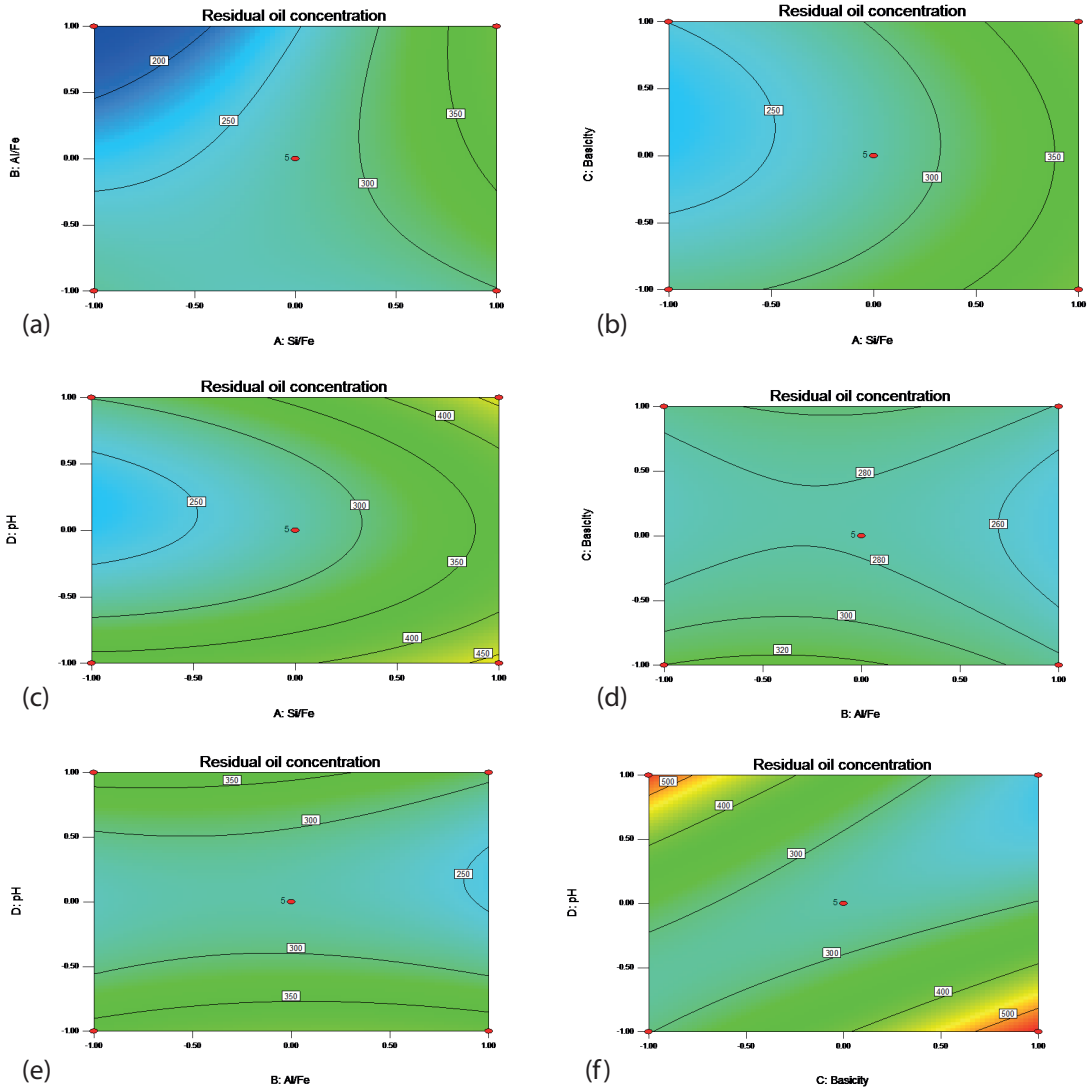

Fig. 4. Mutual effect of Si/Fe, Al/Fe, OH–/Fe (basicity) and pH on residual oil concentration: (a) Mutual effect of Si/Fe and Al/Fe, (b) Mutual effect of Si/Fe and basicity, (c) Mutual effect of Si/Fe and pH, (d) Mutual effect of Al/Fe and basicity, (e) Mutual effect of Al/Fe and pH, (f) Mutual effect of basicity and pH.

Table 4
Measured and calculated values for confirmation experiments

Run	Si/Fe (X_1)	Al/Fe (X_2)	OH^-/Fe (X_3)	pH (X_4)	Residual oil concentration ($mg \cdot L^{-1}$)	
					Measured	Calculated
30	0.98	–1	–1	–0.78	263.6	274.8
31	1	–0.97	–1	0.77	265.8	278.3
32	0.98	–1	–0.96	–0.83	266.7	276.8
33	1	–0.96	–1	–0.83	271.5	279.1

3.8. Effect of pH on the removal of COD and oil

Fig. 7 shows the effect of pH on the flocculation efficiency of oily wastewater. As shown in Fig. 7(a), the increase in pH from 4 to 7 increased the COD removal efficiency. However, when the pH value was in the range of 7–10, the COD removal rate began to decrease. The maximum COD removal rates were 95.4% and 87.9% for PAFSi and PAFS at pH 7, respectively. Fig. 7(b) shows the effect of pH on oil removal. With the increase in pH, the removal rate of oil increased slightly and then decreased sharply for both PAFSi and PAFS. The maximum removal rates of oil by PAFSi and PAFS at pH 7

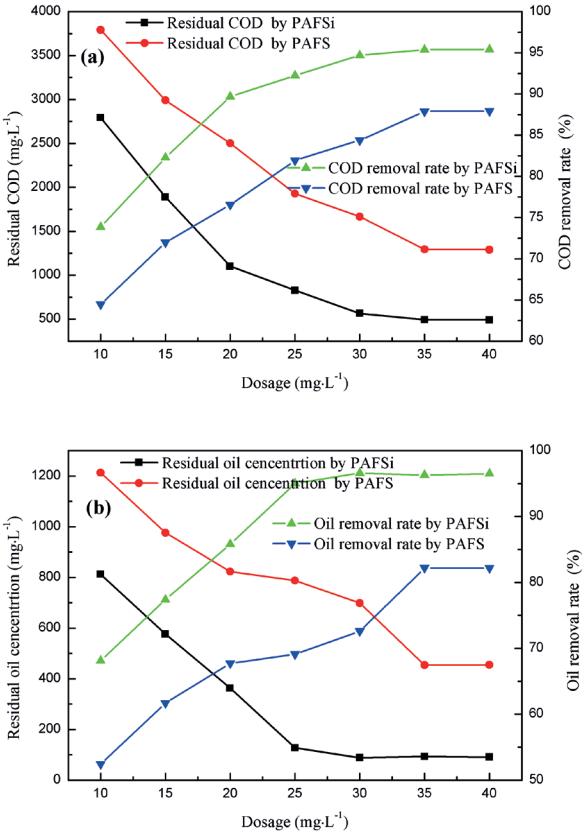

Fig. 5. Effect of dosage on flocculation efficiency of oil wastewater: (a) Effect of dosage on COD removal, (b) Effect of dosage on oil removal.

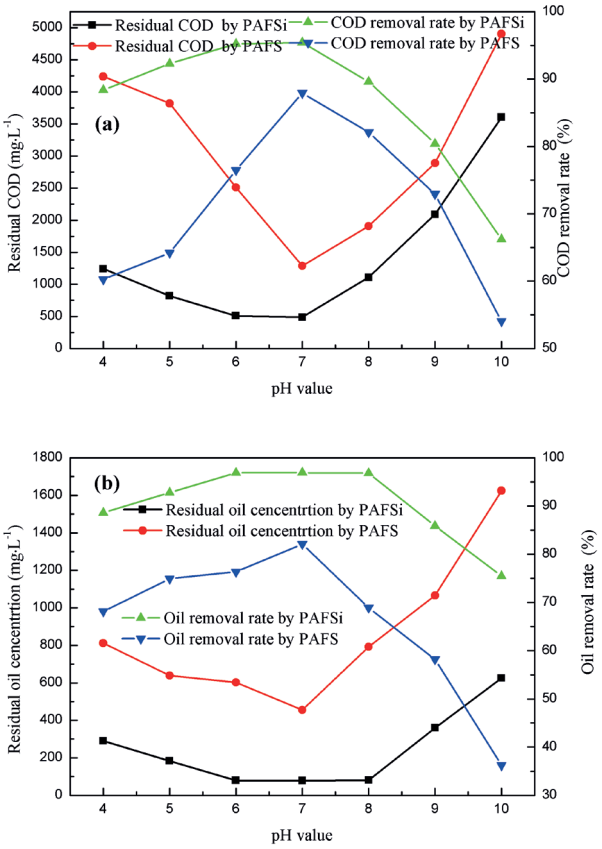

Fig. 7. Effect of pH on flocculation efficiency of oil wastewater: (a) Effect of dosage on COD removal, (b) Effect of dosage on oil removal.

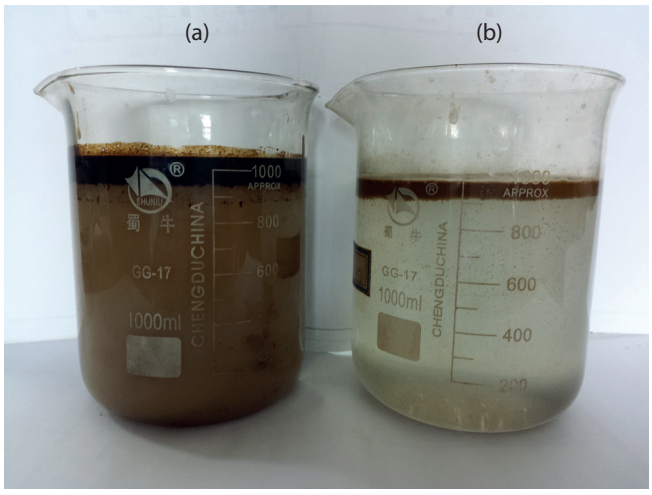

Fig. 6. Photographs of flocculation result of oil wastewater: (a) before flocculation and (b) after flocculation.

were 96.9% and 82.1%, respectively, with residual oil concentration of 77.6 and 455.9 mg·L^{-1}, respectively. As illustrated in Fig. 7(b), pH 6–8 was the optimal pH range for oil removal by PAFSi, indicating that PAFSi had a larger efficiency range than PAFS. Therefore, the optimum pH value to maximize the performance of coagulation by PAFSi was 6–8.

As pH increased, COD and oil removal increased initially and then decreased after pH 7. The best flocculation effect was obtained at pH 7. When pH was low, some coagulants were hydrolyzed into Al^{3+} and Fe^{3+} by H^+, resulting in the decrease in the flocculation–coagulation efficiency of PAFSi [40,41]. Meanwhile, a large amount of H^+ in the wastewater caused the suspended colloid particles to become positively charged, which led to the re-stabilization of suspended colloid particles [42]. When pH was high, OH^- was conducive to reacting with PAFSi to form $Fe(OH)_3$ precipitate, thus reducing the effectiveness of PAFSi [43]. The large amount of OH^- led to the surface of suspended colloid particles being seriously negatively charged. Consequently, the dosage of PAFSi was insufficient to neutralize the negatively charged surface of suspended colloid particles and thus led to low flocculation–coagulation efficiency [44].

4. Conclusions

The preparation and characterization of PAFSi for the treatment of high-concentration oil-containing wastewater were systematically investigated. The main conclusions from this study are as follows:

- The XRD spectrum proved that the addition of silicic acid changed the manner of accumulation and crystallization of the original polymeric ferric sulfate; this change

resulted in the formation of a new multi-hydroxyl polymer with good stability in long-term storage. FTIR analysis indicated that several possible chemical bonds, such as –OH, Fe–OH, Al–OH, Fe–O–Si, and Al–O–Si, were introduced in PAFSi. These bonds resulted in a new composite coagulant with highly charged polyhydroxy complexes. The results of SEM showed that PAFS presented branched and flake structures with high fractal dimensions.

- RSM was utilized to optimize the process and evaluate the interactions and effects of the four main influential factors, namely Si/Fe, Al/Fe, OH^-/Fe, and pH, on treatment efficiency in terms of residual oil concentration. An optimal condition of Si/Fe of 1:1.36, Al/Fe of 1:7.92, OH^-/Fe of 1.09:1, and pH of 2.38 was obtained from the optimization procedure. The confirmation experiments demonstrated that RSM was effective in modeling and optimizing the preparation procedure. This method was evaluated by the coagulation–flocculation process for the treatment of high-concentration oil-containing wastewater.
- The coagulation–flocculation tests demonstrated that PAFSi exhibited better flocculation ability to remove COD and oil than PAFS. The maximum oil removal efficiency of PAFSi could reach 96.9% at a dosage of 25 $mg \cdot L^{-1}$ and pH of 7.

Acknowledgments

This research was supported by the National Natural Science Foundation of China (No. 51508268), the Natural Science Foundation of the Jiangsu Province in China (No. BK20150951), and China Postdoctoral Science Foundation (No. 2016M591835). This research was also supported by Natural Science Foundation of the Jiangsu Higher Education Institution of China (12KJA610001) and Science and Technology Program of the Ministry of Housing and Urban-Rural Development of China (2014-K7-010).

References

[1] S. Jamaly, A. Giwa, S.W. Hasan, Recent improvements in oily wastewater treatment: progress, challenges, and future opportunities, J. Environ. Sci., 37 (2015) 15–30.
[2] X. Zhao, T. Yang, L. Liu, X. Zhang, L. Fan, Y. Huang, Effect of aluminum speciation on silica removal during coagulation of heavy-oil wastewater using polyaluminum chloride, Desal. Wat. Treat., 25 (2016) 11789–11799.
[3] K. Tong, Y. Zhang, P.K. Chu, Evaluation of calcium chloride for synergistic emulsification of super heavy oil wastewater, Colloids Surf., A, 419 (2013) 46–52.
[4] Z. Yang, B. Gao, C. Li, Q. Yue, B. Liu, Synthesis and characterization of hydrophobically associating cationic polyacrylamide, Chem. Eng. J., 161 (2010) 27–33.
[5] X. Wang, S. Xu, Y. Tan, J. Du, J. Wang, Synthesis and characterization of a porous and hydrophobic cellulose-based composite for efficient and fast oil–water separation, Carbohydr. Polym., 140 (2016) 188–194.
[6] W. Wang, Z. Ye, F. Li, Removal of oil from simulated oilfield wastewater using modified coal fly ashes, Desal. Wat. Treat., 21 (2016) 9644–9650.
[7] J. Zhong, X. Sun, C. Wang, Treatment of oily wastewater produced from refinery processes using flocculation and ceramic membrane filtration, Sep. Purif. Technol., 32 (2003) 93–98.
[8] S. Safari, M.A. Aghdam, H.R. Kariminia, Electrocoagulation for COD and diesel removal from oily wastewater, Int. J. Environ. Sci. Technol., 13 (2016) 231–242.
[9] N. Habashi, N. Mehrdadi, A. Mennerich, A. Alighardashi, A. Torabian, Hydrodynamic cavitation as a novel approach for pretreatment of oily wastewater for anaerobic co-digestion with waste activated sludge, Ultrason. Sonochem., 31 (2016) 362–370.
[10] M. Tir, N. Moulai-Mostefa, Optimization of oil removal from oily wastewater by electrocoagulation using response surface method, J. Hazard. Mater., 158 (2008) 107–115.
[11] S. Ibrahim, S. Wang, H.M. Ang, Removal of emulsified oil from oily wastewater using agricultural waste barley straw, Biochem. Eng. J., 49 (2010) 78–83.
[12] T. Yang, B. Qiao, G. Li, Q. Yang, Improving performance of dynamic membrane assisted by electrocoagulation for treatment of oily wastewater: effect of electrolytic conditions, Desalination, 363 (2015) 134–143.
[13] T. Lu, D. Qi, H. Zhao, Y. Cheng, Synthesis of hydrophobically modified flocculant by aqueous dispersion polymerization and its application in oily wastewater treatment, Polym. Eng. Sci., 55 (2014) 1–7.
[14] K. Liao, X. Ye, P. Chen, Z. Xu, Biomineralized polypropylene/$CaCO_3$ composite nonwoven meshes for oil/water separation, J. Appl. Polym. Sci., 131 (2014) 39897.
[15] A.L. Ahmad, S. Sumathi, B.H. Hameed, Residual oil and suspended solid removal using natural adsorbents chitosan, bentonite and activated carbon: a comparative study, Chem. Eng. J., 108 (2005) 179–185.
[16] C. Wang, A. Alpatova, K.N. McPhedran, M.G. El-Din, Coagulation/flocculation process with polyaluminum chloride for the remediation of oil sands process-affected water: performance and mechanism study, J. Environ. Manage., 160 (2015) 254–262.
[17] C.E. Santo, V.J.P. Vilar, C.M.S. Botelho, A. Bhatnagar, E. Kumar, R.A.R. Boaventura, Optimization of coagulation–flocculation and flotation parameters for the treatment of a petroleum refinery effluent from a Portuguese plant, Chem. Eng. J., 183 (2012) 117–123.
[18] J. Zhang, B. Jing, S. Fang, M. Duan, Y. Ma, Synthesis and performances for treating oily wastewater produced from polymer flooding of new demulsifiers based on polyoxyalkylated *N*,*N*-dimethylethanolamine, Polym. Adv. Technol., 26 (2015) 190–197.
[19] K. Tong, A. Lin, G. Ji, D. Wang, X. Wang, The effects of adsorbing organic pollutants from super heavy oilwastewater by lignite activated coke, J. Hazard. Mater., 308 (2016) 113–119.
[20] S. Mirshahghassemi, J.R. Lead, Oil recovery from water under environmentally relevant conditions using magnetic nanoparticles, Environ. Sci. Technol., 49 (2015) 11729–11736.
[21] T. Chen, M. Duan, S. Fang, Fabrication of novel superhydrophilic and underwater superoleophobic hierarchically structured ceramic membrane and its separation performance of oily wastewater, Ceram. Int., 42 (2016) 8604–8612.
[22] X. Zhao, L. Liu, Y. Wang, H. Dai, D. Wang, H. Cai, Influences of partially hydrolyzed polyacrylamide (HPAM) residue on the flocculation behavior of oily wastewater produced from polymer flooding, Sep. Purif. Technol., 62 (2008) 199–204.
[23] Y. Liu, Advanced treatment of biologically treated heavy oil wastewater for reuse as boiler feed-water by combining ultrafiltration and nanofiltration, Desal. Wat. Treat., 28 (2016) 13113–13119.
[24] J. Li, D. Li, W. Li, H. She, H. Feng, D. Hu, Facile fabrication of three-dimensional superhydrophobic foam for effective separation of oil and water mixture, Mater. Lett., 171 (2016) 228–231.
[25] Y. Sun, H. Zheng, Z. Xiong, Y. Wang, X. Tang, W. Chen, Y. Ding, Algae removal from raw water by flocculation and the fractal characteristics of flocs, Desal. Wat. Treat., 56 (2015) 894–904.
[26] T.K. Trinh, L.S. Kang, Application of response surface method as an experimental design to optimize coagulation tests, Environ. Eng. Res., 2 (2010) 63–70.
[27] M.A. Bezerra, R.E. Santelli, E.P. Oliveira, L.S. Villar, L.A. Escaleira, Response surface methodology (RSM) as a tool for optimization in analytical chemistry, Talanta, 76 (2008) 965–977.
[28] W. Zhou, B. Gao, Q. Yue, L. Liu, Y. Wang, Al-Ferron kinetics and quantitative calculation of Al(III) species in polyaluminum chloride coagulants, Colloids Surf., A, 278 (2006) 235–240.

[29] H. Dong, B. Gao, Q. Yue, H. Rong, S. Sun, S. Zhao, Effect of Fe (III) species in polyferric chloride on floc properties and membrane fouling in coagulation–ultrafiltration process, Desalination, 335 (2014) 102–107.
[30] G. Zhu, H. Zheng, Z. Zhang, T. Tshukudu, P. Zhang, X. Xiang, Characterization and coagulation–flocculation behavior of polymeric aluminum ferric sulfate (PAFS), Chem. Eng. J., 178 (2011) 50–59.
[31] W. Chen, H. Zheng, J. Guo, F. Li, X. Tang, B. Liu, Y. Zhou, Preparation and characterization of a composite coagulant: polyferric titanium sulfate, Water Air Soil Pollut., 227 (2016) 79.
[32] G. Zhu, H. Zheng, W. Chen, W. Fan, P. Zhang, T. Tshukudu, Preparation of a composite coagulant: polymeric aluminum ferric sulfate (PAFS) for wastewater treatment, Desalination, 285 (2012) 315–323.
[33] H. Zheng, G. Zhu, S. Jiang, T. Tshukudu, X. Xiang, P. Zhang, Q. He, Investigations of coagulation–flocculation process by performance optimization, model prediction and fractal structure of flocs, Desalination, 269 (2011) 148–156.
[34] H. Wu, R. Yang, R. Li, C. Long, H. Yang, A. Li, Modeling and optimization of the flocculation processes for removal of cationic and anionic dyes from water by an amphoteric grafting chitosan-based flocculant using response surface methodology, Environ. Sci. Pollut. Res., 22 (2015) 13038–13048.
[35] J. Wang, Y. Chen, Y. Wang, S. Yuan, H. Yu, Optimization of the coagulation-flocculation process for pulp mill wastewater treatment using a combination of uniform design and response surface methodology, Water Res., 45 (2011) 5633–5640.
[36] H. Zheng, J. Ma, J. Zhai, C. Zhu, X. Tang, Y. Liao, L. Qian, Y. Sun, Optimization of flocculation process by response surface methodology for diethyl phthalate removal using anionic polyacrylamide, Desal. Wat. Treat., 28 (2014) 5390–5400.
[37] T. Sun, C. Sun, G. Zhu, X. Miao, C. Wu, S. Lv, W. Li, Preparation and coagulation performance of poly-ferric-aluminum-silicate-sulfate from fly ash, Desalination, 268 (2011) 270–275.
[38] T. Lu, H. Zhao, D. Qi, Y. Chen, Synthesis of a novel amphiphilic and cationic chitosan-based flocculant for efficient treatment of oily wastewater, Adv. Polym. Tech., 34 (2015) 21502.
[39] Y. Sun, H. Zheng, M. Tan, Y. Wang, X. Tang, L. Feng, X. Xiang, Synthesis and characterization of composite flocculant PAFS–CPAM for the treatment of textile dye wastewater, J. Appl. Polym. Sci., 131 (2014) 40062.
[40] K. Yang, Y. Li, Y. Chen, Removal of oil and Cr(VI) from wastewater using modified pectin flocculants, J. Environ. Eng., 140 (2014) 472–472.
[41] J. Zhang, B. Jing, G. Tan, L. Zhai, S. Fang, Y. Ma, Comparison of performances of different types of clarifiers for the treatment of oily wastewater produced from polymer flooding, Can. J. Chem. Eng., 93 (2015) 1288–1294.
[42] R. Li, J. Pan, W. Qin, J. Yang, Y. He, Effect of pH on characterization and coagulation performance of poly-silicic-cation coagulant, Desalination, 351 (2014) 37–42.
[43] Y. Zeng, J. Park, Characterization and coagulation performance of a novel inorganic polymer coagulant—poly-zinc-silicate-sulfate, Colloids Surf., A, 334 (2009) 147–154.
[44] A.L. Ahmad, S. Sumathi, B.H. Hameed, Coagulation of residue oil and suspended solid in palm oil mill effluent by chitosan, alum and PAC, Chem. Eng. J., 118 (2006) 99–105.